PHYSICAL REVIEW D **96,** 091103(R) (2017)

Limiting neutrino magnetic moments with Borexino Phase-II solar neutrino data

M. Agostini,[1,8] K. Altenmüller,[2] S. Appel,[2] V. Atroshchenko,[3] Z. Bagdasarian,[4] D. Basilico,[5] G. Bellini,[5] J. Benziger,[6] D. Bick,[7] G. Bonfini,[8] D. Bravo,[5,9] B. Caccianiga,[5] F. Calaprice,[10] A. Caminata,[11] S. Caprioli,[5] M. Carlini,[8] P. Cavalcante,[8,9] A. Chepurnov,[12] K. Choi,[13] L. Collica,[5] D. D'Angelo,[5] S. Davini,[11] A. Derbin,[14] X. F. Ding,[1,8] A. Di Ludovico,[10] L. Di Noto,[11] I. Drachnev,[1,14,8] K. Fomenko,[15] A. Formozov,[15,5,16] D. Franco,[17] F. Froborg,[10] F. Gabriele,[8] C. Galbiati,[10] C. Ghiano,[8] M. Giammarchi,[5] A. Goretti,[10] M. Gromov,[16] D. Guffanti,[1,8] C. Hagner,[7] T. Houdy,[17] E. Hungerford,[18] Aldo Ianni,[8,*] Andrea Ianni,[10] A. Jany,[19] D. Jeschke,[2] V. Kobychev,[20] D. Korablev,[15] G. Korga,[18] D. Kryn,[17] M. Laubenstein,[8] E. Litvinovich,[3,21] F. Lombardi,[8,†] P. Lombardi,[5] L. Ludhova,[4,22] G. Lukyanchenko,[3] L. Lukyanchenko,[3] I. Machulin,[3,21] G. Manuzio,[11] S. Marcocci,[1,11,8] J. Martyn,[23] E. Meroni,[5] M. Meyer,[24] L. Miramonti,[5] M. Misiaszek,[19] V. Muratova,[14] B. Neumair,[2] L. Oberauer,[2] B. Opitz,[7] V. Orekhov,[3] F. Ortica,[25] M. Pallavicini,[11] L. Papp,[2] Ö. Penek,[4,22] N. Pilipenko,[14] A. Pocar,[26] A. Porcelli,[23] G. Ranucci,[5] A. Razeto,[8] A. Re,[5] M. Redchuk,[4,22] A. Romani,[25] R. Roncin,[8,17] N. Rossi,[8] S. Schönert,[2] D. Semenov,[14] M. Skorokhvatov,[3,21] O. Smirnov,[15] A. Sotnikov,[15] L. F. F. Stokes,[8] Y. Suvorov,[27,3] R. Tartaglia,[8] G. Testera,[11] J. Thurn,[24] M. Toropova,[3] E. Unzhakov,[14] A. Vishneva,[15] R. B. Vogelaar,[9] F. von Feilitzsch,[2] H. Wang,[27] S. Weinz,[23] M. Wojcik,[19] M. Wurm,[23] Z. Yokley,[9] O. Zaimidoroga,[15] S. Zavatarelli,[11] K. Zuber,[24] and G. Zuzel[19]

(The Borexino collaboration)

[1]*Gran Sasso Science Institute, 67100 L'Aquila, Italy*
[2]*Physik-Department and Excellence Cluster Universe, Technische Universität München, 85748 Garching, Germany*
[3]*National Research Centre Kurchatov Institute, 123182 Moscow, Russia*
[4]*Institut für Kernphysik, Forschungszentrum Jülich, 52425 Jülich, Germany*
[5]*Dipartimento di Fisica, Università degli Studi e INFN, 20133 Milano, Italy*
[6]*Chemical Engineering Department, Princeton University, Princeton, New Jersey 08544, USA*
[7]*Institut für Experimentalphysik, Universität Hamburg, 22761 Hamburg, Germany*
[8]*INFN Laboratori Nazionali del Gran Sasso, 67010 Assergi (AQ), Italy*
[9]*Physics Department, Virginia Polytechnic Institute and State University, Blacksburg, Virginia 24061, USA*
[10]*Physics Department, Princeton University, Princeton, New Jersey 08544, USA*
[11]*Dipartimento di Fisica, Università degli Studi e INFN, 16146 Genova, Italy*
[12]*Moscow State University Skobeltsyn Institute of Nuclear Physics, 119234 Moscow, Russia*
[13]*Department of Physics and Astronomy, University of Hawaii, Honolulu, Hawaii 96822, USA*
[14]*St. Petersburg Nuclear Physics Institute NRC Kurchatov Institute, 188350 Gatchina, Russia*
[15]*Joint Institute for Nuclear Research, 141980 Dubna, Russia*
[16]*Moscow State University, Physics Department, 119234 Moscow, Russia*
[17]*AstroParticule et Cosmologie, Université Paris Diderot, CNRS/IN2P3, CEA/IRFU, Observatoire de Paris, Sorbonne Paris Cité, 75205 Paris Cedex 13, France*
[18]*Department of Physics, University of Houston, Houston, Texas 77204, USA*
[19]*M. Smoluchowski Institute of Physics, Jagiellonian University, 30348 Krakow, Poland*
[20]*Kiev Institute for Nuclear Research, 03028 Kiev, Ukraine*
[21]*National Research Nuclear University MEPhI (Moscow Engineering Physics Institute), 115409 Moscow, Russia*
[22]*RWTH Aachen University, 52062 Aachen, Germany*
[23]*Institute of Physics and Excellence Cluster PRISMA, Johannes Gutenberg-Universität Mainz, 55099 Mainz, Germany*
[24]*Department of Physics, Technische Universität Dresden, 01062 Dresden, Germany*
[25]*Dipartimento di Chimica, Biologia e Biotecnologie, Università degli Studi e INFN, 06123 Perugia, Italy*
[26]*Amherst Center for Fundamental Interactions and Physics Department, University of Massachusetts, Amherst, Massachusetts 01003, USA*
[27]*Physics and Astronomy Department, University of California Los Angeles (UCLA), Los Angeles, California 90095, USA*

(Received 14 August 2017; published 29 November 2017)

[*]Also at Laboratorio Subterráneo de Canfranc, Paseo de los Ayerbe S/N, 22880 Canfranc Estacion Huesca, Spain.
[†]Present address: Physics Department, University of California, San Diego, California 92093, USA.

A search for the solar neutrino effective magnetic moment has been performed using data from 1291.5 days exposure during the second phase of the Borexino experiment. No significant deviations from the expected shape of the electron recoil spectrum from solar neutrinos have been found, and a new upper limit on the effective neutrino magnetic moment of $\mu_\nu^{\rm eff} < 2.8 \times 10^{-11}\ \mu_B$ at 90% C.L. has been set using constraints on the sum of the solar neutrino fluxes implied by the radiochemical gallium experiments. Using the limit for the effective neutrino moment, new limits for the magnetic moments of the neutrino flavor states, and for the elements of the neutrino magnetic moments matrix for Dirac and Majorana neutrinos, are derived.

DOI: 10.1103/PhysRevD.96.091103

I. INTRODUCTION

Neutrinos produced in the Sun are a unique source of information with regards to their physical properties. Besides the study of well-established neutrino oscillations they can also be used to look for an anomalous magnetic moment and other electromagnetic properties of neutrinos [1–6]. The neutrino magnetic moment in the standard electroweak theory (SM), when extended to include neutrino mass, is proportional to the neutrino mass [7–12],

$$\mu_\nu = \frac{3 m_e G_F}{4\pi^2\sqrt{2}} m_\nu \mu_B \approx 3.2 \times 10^{-19} \left(\frac{m_\nu}{1\ \text{eV}}\right)\mu_B, \quad (1)$$

where $\mu_B = \frac{eh}{4\pi m_e}$ is the Bohr magneton, m_e is the electron mass, and G_F is the Fermi coupling constant. The known upper limit on the neutrino masses m_ν leads to μ_ν less than $10^{-18}\mu_B$, which is roughly 8 orders of magnitude lower than existing experimental limits. The most stringent laboratory bounds on μ_ν are obtained by studying (ν, e) elastic scattering of solar neutrinos and reactor antineutrinos. The Super-Kamiokande Collaboration achieved a limit of $3.6 \times 10^{-10}\ \mu_B$ (90% C.L.) by fitting day/night solar neutrino spectra above 5 MeV. With additional information from other solar neutrino and KamLAND experiments a limit of $1.1 \times 10^{-10}\ \mu_B$ (90% C.L.) was obtained [13]. The Borexino collaboration reported the best current limit on the effective magnetic moment of $5.4 \times 10^{-11}\ \mu_B$ (90% C.L.) using the electron recoil spectrum from ^{7}Be solar neutrinos [14].

The best limit from reactor antineutrinos is 2.9×10^{-11} μ_B (90% C.L.) [15]. More stringent limits on the neutrino magnetic moment of up to $\sim 10^{-12}\mu_B$ come from astrophysical observations [16,17]. The complete historical record of searching for the neutrino magnetic moment can be found in [18].

Though experimental bounds on μ_ν are far from the value predicted by the extended SM, in more general models, for example with right-handed bosons or with an extended sector of scalar particles, the magnetic moment can be proportional to the mass of charged leptons and can have values close to the experimental limits reported. In more general models the proportionality between the neutrino mass and its magnetic moment does not hold.

In this paper, we report results of a search for neutrino magnetic moments using data collected during the Borexino Phase-II campaign. The Borexino detector is located in the Gran Sasso National Laboratory, Italy. Borexino detects solar neutrinos via the elastic scattering off electrons. The recoil electrons are detected via scintillation light, which carries the energy and position information. The mass of the scintillator (PC + PPO) is 278 tons. Events are selected within a fiducial volume (FV) corresponding to approximately 1/4 of the scintillator volume in order to provide an "active shield" against external backgrounds. Detailed descriptions of the detector can be found in [19,20].

In the SM, the scattering of a neutrino with a nonzero magnetic moment is determined by both a weak interaction and a single-photon exchange term. The latter changes the helicity of the final neutrino state. This means that the amplitudes of the weak and electromagnetic scattering do not interfere, at least at the level of $\sim m_\nu/E_\nu$, and the total cross section is the sum of the two.

Neutrino mixing means that the coupling of the neutrino mass eigenstates i and j to an electromagnetic field is characterized by a 3×3 matrix of the magnetic (and electric) dipole moments μ_{ij}. For Majorana neutrinos the matrix μ_{ij} is antisymmetric and only transition moments are allowed, while for Dirac neutrinos μ_{ij} is a general 3×3 matrix. The electromagnetic contribution to the ν–e scattering cross section is proportional to the square of the effective magnetic moment $\mu_{\rm eff}$,

$$\frac{d\sigma_{\rm EM}}{dT_e}(T_e, E_\nu) = \pi r_0^2 \mu_{\rm eff}^2 \left(\frac{1}{T_e} - \frac{1}{E_\nu}\right), \quad (2)$$

where $\mu_{\rm eff}$ is measured in μ_B units and depends on the components of the neutrino moments matrix μ_{ij}, T_e is electron recoil energy, and $r_0 = 2.818 \times 10^{-13}$ cm is the classical electron radius.

The energy dependence for the magnetic and weak scattering cross sections differs significantly; for $T_e \ll E_\nu$ their ratio is proportional to $1/T_e$ and the sensitivity of the experiment to the magnetic moment strongly depends on the threshold of detection. This makes the low-energy threshold of Borexino suitable for a neutrino magnetic moment search.

II. DATA SELECTION AND ANALYSIS

The data used for the analysis were collected from December 14, 2011 to May 21, 2016 with a live-time of 1291.5 days. Events were selected following the procedure optimized for the new solar neutrino analysis [21]: all events within 2 ms of any muon were rejected, while a dead time of 300 ms was applied after muons crossing the inner detector; decays due to radon daughters occurring before ^{214}Bi-^{214}Po delayed coincidences are vetoed; events must be reconstructed within the FV defined by the following conditions: $R \leq 3.021$ m and $|Z| \leq 1.67$ m where R is the reconstructed distance to the detector center and Z is the reconstructed vertical coordinate. The cuts reduce the live-time to 1270.6 days, and the total FV exposure corresponds to 263.7 tonne $\cdot$ y.

The model function fitted to the data has been restricted to the same components used in the solar neutrino analysis of the second phase (see [21]), namely ^{14}C, ^{85}Kr, ^{210}Bi β-decay shapes, the β^+ spectrum of the cosmogenic ^{11}C, the monoenergetic α peak from ^{210}Po decays, γ-rays from external sources and the electron recoil spectra from ^{7}Be, pp, pep and the CNO cycle neutrinos. Other backgrounds and solar neutrino components have a negligible impact on the total spectrum. Compared to previous solar neutrino analyses ([14,22–24]) an extended energy region was used, including both pp and ^{7}Be neutrino contributions in the same fit. In addition, the upper limit of the fit is set above the ^{11}C end point, which helps to constrain the resolution behavior at the high end of the energy spectrum [21].

The analytical model used to describe the data is an improved version of the one described in [24] with the goal of enlarging the fitting energy range. The principal changes concern the nonlinearities of the energy scale and the addition of a resolution parameter to describe the low-energy region. The former parameter was first used in the pp-neutrino flux analysis [25]. The energy estimator N_p used is the number of photomultiplier tubes (PMTs) triggered in each event (window of 230 ns) the same as in [25] but normalized to 2000 PMTs. This is different from the earlier pp neutrino analysis (408 days of data) where non-normalized energy variables were used; normalization is needed in order to compensate for significant degradation of resolution for non-normalized variables during the longer period.

In order to correct for the nonstatistical fluctuations in the data arising from rebinning an intrinsically integer variable N_p a correction at each bin was applied, calculated on the basis of the known number of functioning PMTs at each moment. The model is discussed in [21]; more details will be presented in a devoted paper [26].

The analytical model function has in total 15 free parameters. The free parameter describing the energy scale is the light yield; two free parameters are used for resolution. Other parameters describe the rates of dominant backgrounds, namely ^{14}C (constrained to the value determined by analyzing an independent sample of ^{14}C events selected with low threshold, see [25] for more detail), ^{85}Kr, ^{210}Bi, ^{11}C, ^{210}Po peak, and external backgrounds [responses from the ^{208}Tl and ^{214}Bi γ-rays modeled with Monte Carlo method (MC)]. The pp and ^{7}Be interaction rates represent the solar neutrino parameters. The remaining free parameters describe the position and width of the ^{210}Po α-peak, and the starting point of the ^{11}C β^+-spectrum (corresponding to two annihilation gammas of 511 keV) as independent calibration does not provide the necessary precision to have them fixed or constrained.

The pep and ^{8}B solar neutrino contributions were kept fixed according to the standard solar model (SSM) predictions and the uncertainty of the prediction contributed to the systematics as described in Sec. III. The minor contribution from external ^{40}K γ-rays was fixed too.

Other parameters of the model are tuned either using MC modeling or independent measurements and calibrations; for details see [21,26,27]. They correspond to parameters describing the energy scale nonlinearities: the ionization quenching parameter, the contribution of the Cherenkov radiation, the geometric correction to the energy scale, the effective fraction of the single electron response under the threshold, and an additional parameter in the resolution description (quadratic with respect to the energy estimator). Special care is taken to describe the pileup events. The same approach is adopted as the one developed for the pp-neutrino analysis [25], where the synthetic pileup is constructed by overlapping real events with randomly sampled data of the same time length.

The ^{210}Bi background and the CNO neutrino spectra are strongly anticorrelated as they have similar spectral shapes. Their sum is constrained by the total number of events in the region between the ^{7}Be Compton-like shoulder and the ^{11}C spectrum (see Fig. 1), which is mostly free from other backgrounds. As the CNO contribution is masked by the larger ^{210}Bi rate, the CNO neutrino rate is fixed to the SSM + MSW prediction without considering electromagnetic contribution. We used both high and low metallicity variants of the SSM; the difference in results was included in the systematics. The electromagnetic term did not affect the fit results with respect to the CNO contribution as it was absorbed by the ^{210}Bi component.

The likelihood profile as a function of μ_ν^{eff} is obtained from the fit with the addition of the electromagnetic component for ^{7}Be and pp neutrinos keeping μ_ν^{eff} fixed at each point. The electromagnetic contribution from all other solar neutrino fluxes is negligible and is not considered in the fit. Including the electromagnetic component described by (2) in the pp-neutrino cross section leads to a decrease of the pp-neutrino flux in the fit, compensating for the increase in the total cross section. Another important correlation arises from the presence of ^{85}Kr in the fitting function. An increase in the ^{7}Be rate due to the electromagnetic interactions is compensated for by a decrease in

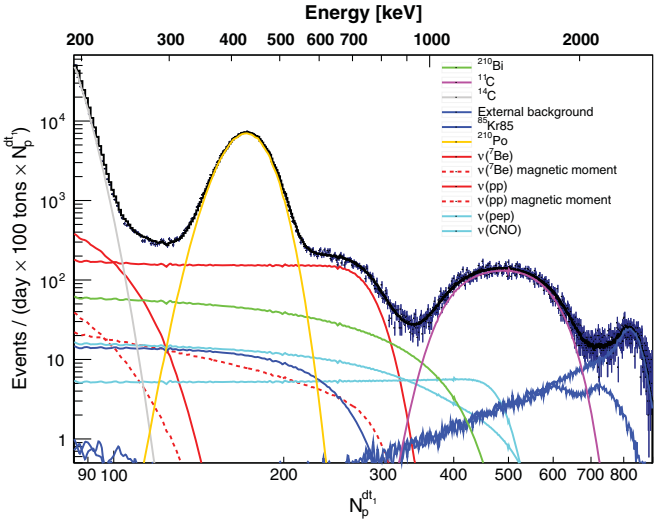

FIG. 1. Spectral fit with the neutrino effective moment fixed at $\mu_\nu^{\rm eff} = 2.8 \times 10^{-11}\mu_B$ (note the scale is double logarithmic to underline the contributions at lower energies). The fitting curves for $\mu_\nu^{\rm eff} = 2.8 \times 10^{-11}\mu_B$ and $\mu_\nu^{\rm eff} = 0$ are visually indistinguishable.

the ^{85}Kr counting rate. These two correlations in the fit decrease the overall sensitivity to the magnetic moment. The contribution from ^{85}Kr could be constrained from an independent measurement using a delayed coincidence, but the combination of a very low branching ratio of 0.4%, low tagging efficiency (∼18%), and a relatively low ^{85}Kr rate lead to very low statistics in the coincidence branch [21]. As a result, constraining ^{85}Kr does not improve the sensitivity. On the other hand, the correlation between the magnetic moment and the pp-neutrino flux can be constrained by applying the results from radiochemical experiments, which are independent of the electromagnetic properties of neutrinos, to the sum of the neutrino fluxes detected in Borexino.

The radiochemical constraints are based on the results from [28]. The measured neutrino signal in gallium experiments expressed in solar neutrino units (SNU) is

$$R = \sum_i R_i^{Ga} = \sum_i \Phi_i \int_{E_{th}}^{\infty} s_i^{\odot}(E) P_{ee}(E) \sigma(E) dE$$
$$= \sum_i \Phi_i \langle \sigma_i^{\odot} \rangle = 66.1 \pm 3.1 \text{SNU}, \quad (3)$$

where R is the total neutrino rate, R_i is the contribution of the ith solar neutrino flux to the total rate, Φ_i is the neutrino flux from ith reaction, $s_i^{\odot}(E)$ is the shape of the corresponding neutrino spectrum in the Sun, $P_{ee}(E)$ is the electron neutrino survival probability for neutrinos with energy E, and $\sigma(E)$ is the total cross section of the neutrino interaction with Ga which has a threshold of $E_{th} = 233$ keV.

If applied to Borexino the radiochemical constraint takes the form

$$\sum_i \frac{R_i^{Brx}}{R_i^{\rm SSM}} R_i^{Ga} = (66.1 \pm 3.1 \pm \delta_R \pm \delta_{FV}) \text{SNU} \quad (4)$$

where the expected gallium rates R_i^{Ga} are estimated using new survival probabilities of P_{ee} based on values from [18] (therefore giving a new estimate for $\langle \sigma_i^{\odot} \rangle$), $\frac{R_i^{Brx}}{R_i^{\rm SSM}}$ is the ratio of the corresponding Borexino measured rate to its SSM prediction within the MSW/LMA oscillation scenario. We used the same SSM predictions for Borexino and the gallium experiments to avoid rescaling the gallium expected rates. The total deviation from the measured value should naturally include the additional theoretical error $\delta_R \simeq 4\%$ from the uncertainty in estimating the single rates contributing to the gallium experiments, and the uncertainty of the Borexino FV selection $\delta_{FV} \simeq 1\%$.

Applying the radiochemical constraint (4) to the fit as an additional penalty term, the analysis of the likelihood profile gives a limit of $\mu_\nu^{\rm eff} < 2.6 \times 10^{-11}\mu_B$ at 90% C.L. for the effective magnetic moment of neutrinos using the standard fit conditions (230 ns time window energy variable, synthetic pileup, high metallicity SSM). Without radiochemical constraints the limit is weaker $\mu_\nu^{\rm eff} < 4.0 \times 10^{-11}\mu_B$ at 90% C.L. and is not used in the present analysis. An example of the spectral fit is presented in Fig. 1.

III. SYSTEMATICS STUDY

The systematics have been checked following the approach developed for other Borexino data analyses [25,29]. The main contributions to the systematics comes from the difference in results depending on the choice of energy estimator and the approach used for the pileup modeling. The energy estimators used in the analysis are the number of PMTs triggered within a time window of 230 and 400 ns. The pileup can be reproduced by either convolving the model spectra with the data acquired from the random trigger in the corresponding time window or by constructing a synthetic spectral component as described in [25]. Since the pep- and CNO-neutrino rates are fixed to the SSM predictions, the different rates corresponding to high/low metallicity models are also accounted for in the systematics. Further study included varying the fixed parameters within their expected errors.

The resulting likelihood profile is the weighted sum of the individual profiles of each fit configuration. Initially, the same weights are used for the pileup and SSM choice, assuming equal probabilities for all four possibilities. Further weights are assigned proportionally to the maximum likelihood of each profile, therefore taking into account the quality of the realization of the model with a given set of parameters. Accounting for the systematic uncertainties the limit on the effective neutrino magnetic moment reduces to $\mu_\nu^{\rm eff} < 2.8 \times 10^{-11}\ \mu_B$ at 90% C.L. The corresponding likelihood profile is shown in Fig. 2.

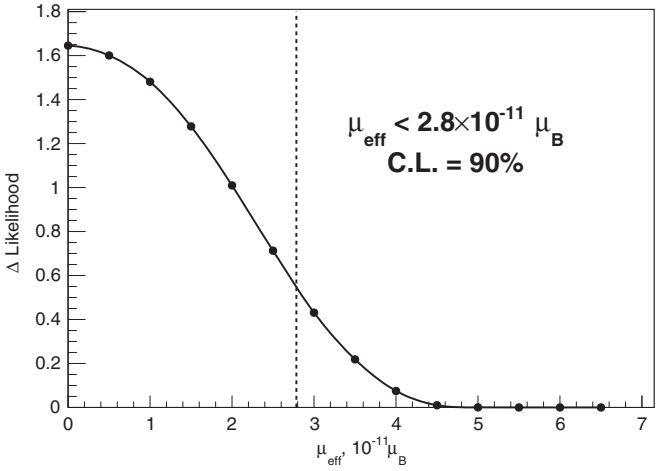

FIG. 2. Resulting weighted likelihood profile used to estimate the limit on the neutrino magnetic moment. The profile does not follow the Gaussian distribution as it is flatter initially and goes to 0 faster than the normal distribution. The limit corresponds to 90% of the total area under the curve. Note that unphysical values of $\mu_\nu^{\rm eff} < 0$ are not considered.

IV. MASS EIGENSTATES BASIS

Since neutrinos are a mixture of mass eigenstates the effective magnetic moment for neutrino-electron scattering is

$$\mu_{\rm eff}^2 = \sum_j \left| \sum_k \mu_{kj} A_k(E_\nu, L) \right|^2, \tag{5}$$

where μ_{jk} is an element of the neutrino electromagnetic moments matrix and $A_k(E_\nu, L)$ is the amplitude of the k-mass state at the point of scattering [30]. For the Majorana neutrino, only the transition moments are nonzero, while the diagonal elements of the matrix are equal to 0 due to CPT conservation. For the Dirac neutrino, all matrix elements may have nonzero values. The effective magnetic moment can be expanded both in terms of the mass eigenstates (this is more natural) or the flavor eigenstates. Under the assumption that $\theta_{13} = 0$, the form of the effective magnetic moment for the MSW oscillation solution has been investigated in [5,31]. The analysis of Majorana transition neutrino magnetic moments taking into account the nonzero value of the angle θ_{13} was first performed in [32].

In the general case the expression for the effective magnetic moment in the mass eigenstate basis will have a complex form consisting of interference terms $\propto \mu_{jk}\mu_{ik}$. Without significant omissions the solar neutrinos arriving at the Earth can be considered as an incoherent mixture of mass eigenstates [5,33]. In the case of Dirac neutrinos assuming that only diagonal magnetic moments μ_{ii} are nonvanishing,

$$\mu_{\rm eff}^2 = P_{e1}^{3\nu}\mu_{11}^2 + P_{e2}^{3\nu}\mu_{22}^2 + P_{e3}^{3\nu}\mu_{33}^2, \tag{6}$$

where $P_{ei}^{3\nu} = |A_i(E, L)|^2$ is the probability of observing the i-mass state at the scattering point for an initial electron flavor.

In the case of Majorana transition magnetic moments the effective moment is

$$\mu_{\rm eff}^2 = P_{e1}^{3\nu}(\mu_{12}^2 + \mu_{13}^2) + P_{e2}^{3\nu}(\mu_{21}^2 + \mu_{23}^2) + P_{e3}^{3\nu}(\mu_{31}^2 + \mu_{32}^2). \tag{7}$$

For the well-known approximation of three- to two-neutrino oscillation probabilities for solar neutrinos [5], $P_{e1}^{3\nu} = \cos^2\theta_{13}P_{e1}^{2\nu}$, $P_{e2}^{3\nu} = \cos^2\theta_{13}P_{e2}^{2\nu}$ and $P_{e3}^{3\nu} = \sin^2\theta_{13}$, one can get the effective magnetic moment expressed in well-established oscillation parameters in the mass eigenstate basis. Eq. (6) can be rewritten as

$$\mu_{\rm eff}^2 = C_{13}^2 P_{e1}^{2\nu}\mu_{11}^2 + C_{13}^2 P_{e2}^{2\nu}\mu_{22}^2 + S_{13}^2\mu_{33}^2 \tag{8}$$

where $C_{13}^2 \equiv \cos^2\theta_{13}$ and $S_{13}^2 \equiv \sin^2\theta_{13}$, and $P_{e1}^{2\nu} + P_{e2}^{2\nu} = 1$. Similarly, assuming CPT conservation ($\mu_{jk} = \mu_{kj}$) relation (7) for the transition moments can be rewritten as

$$\mu_{\rm eff}^2 = C_{13}^2 P_{e1}^{2\nu}\mu_{12}^2 + (1 - C_{13}^2 P_{e2}^{2\nu})\mu_{13}^2 + (1 - C_{13}^2 P_{e1}^{2\nu})\mu_{23.}^2 \tag{9}$$

In general, $P_{e1}^{2\nu}$ and $P_{e2}^{2\nu}$ (and $P_{ee}^{2\nu}$) depend on the neutrino energy, but in the energy region below 1 MeV the probabilities can be assumed constant. Since $\mu_{\rm eff}^2$ is the sum of positively defined quantities, one can constrain any term in (8) and (9). By using the most probable values of $P_{ee}^{2\nu}$, θ_{12} and θ_{13} [18] one can obtain the following limits from the relation $\mu_{\rm eff} \leq 2.8 \times 10^{-11}\mu_B$:

$$|\mu_{11}| \leq 3.4; \qquad |\mu_{22}| \leq 5.1; \qquad |\mu_{33}| \leq 18.7, \tag{10}$$

$$|\mu_{12}| \leq 2.8; \qquad |\mu_{13}| \leq 3.4; \qquad |\mu_{23}| \leq 5.0, \tag{11}$$

all measured in units of $10^{-11}\mu_B$ and for 90% C.L.

V. LIMITS ON MAGNETIC MOMENTS OF THE NEUTRINO FLAVOR STATES

The effective magnetic moment for the LMA-MSW solution is

$$\mu_{\rm eff}^2 = P^{3\nu}\mu_e^2 + (1 - P^{3\nu})(\cos^2\theta_{23}\cdot\mu_\mu^2 + \sin^2\theta_{23}\cdot\mu_\tau^2), \tag{12}$$

where $P^{3\nu} = \sin^4\theta_{13} + \cos^4\theta_{13}P^{2\nu}$ is the probability that ν_e is detected in its original flavor (survival probability), with $P^{2\nu}$ calculated in the standard 2-neutrino scheme; θ_{13} and θ_{23} are the corresponding mixing angles. Though $P^{2\nu}$ depends on E_ν, the difference between $P^{2\nu}(400) = 0.57$ for a neutrino energy close to the pp-neutrino spectrum end point of 420 keV (only a small fraction of the total pp-neutrino spectrum close to the end point contributes to the sensitive region in our analysis) and $P^{2\nu}(862) = 0.55$ for ^{7}Be neutrinos (higher energy line) is negligible. Moreover, tests performed by "turning on" separately the pp and ^{7}Be neutrino magnetic moments demonstrate that sensitivity to the magnetic moment is dominated by the ^{7}Be-neutrino

contribution. Therefore an estimate of $P^{2\nu} = 0.55$ is used in further calculations.

The limits on the flavor magnetic moment can be obtained from (12) because individual contributions are positive. With $\mu_\nu^{\text{eff}} < 2.8 \times 10^{-11}\mu_B$ and for $\sin^2\theta_{13} = 0.0210 \pm 0.0011$ and $\sin^2\theta_{23} = 0.51 \pm 0.04$ for normal hierarchy (or $\sin^2\theta_{23} = 0.50 \pm 0.04$ for inverted hierarchy) [18] we obtain $\mu_e < 3.9 \times 10^{-11}\mu_B$, $\mu_\mu < 5.8 \times 10^{-11}\mu_B$ and $\mu_\tau < 5.8 \times 10^{-11}\mu_B$, all at 90% C.L.

Because the mass hierarchy is still unknown, the values above were calculated for the choice of hierarchy providing a more conservative limit.

VI. CONCLUSIONS

New upper limits for the neutrino magnetic moments have been obtained using 1291.5 days of data from the Borexino detector. We searched for effects of the neutrino magnetic moments by looking for distortions in the shape of the electron recoil spectrum. A new model independent limit of $\mu_\nu^{\text{eff}} < 2.8 \times 10^{-11}\ \mu_B$ is obtained at 90% C.L. including systematics. The limit is free from uncertainties associated with predictions from the SSM neutrino flux and systematics from the detector's FV and is obtained by constraining the sum of the solar neutrino fluxes using the results from gallium experiments. The limit on the effective neutrino moment for solar neutrinos was used to set new limits on the magnetic moments for the neutrino flavor states and for the elements of the neutrino magnetic moments matrix for Dirac and Majorana neutrinos.

ACKNOWLEDGMENTS

The Borexino program is made possible by funding from INFN (Italy), NSF (USA), BMBF, DFG, HGF and MPG (Germany), RFBR (Grants No. 16-02-01026A, No. 15-02-02117A, No. 16-29-13014 ofi_m, and No. 17-02-00305A) and RSF (Grant No. 17-12-01009) (Russia), JINR Grant No. 17-202-01, and NCN Poland (Grant No. UMO-2013/10/E/ST2/00180). We acknowledge the generous hospitality and support of the Laboratory Nazionali del Gran Sasso (Italy).

[1] M. B. Voloshin, M. I. Vysotskii, and L. B. Okun, Sov. J. Nucl. Phys. **44**, 440 (1986); M. B. Voloshin, M. I. Vysotskii, and L. B. Okun, Sov. Phys. JETP **64**, 446 (1986).
[2] C. S. Lim and W. Marciano, Phys. Rev. D **37**, 1368 (1988).
[3] E. Kh. Akhmedov, Phys. Lett. B **213**, 64 (1988).
[4] H. O. Back *et al.* (Borexino Collaboration), Phys. Lett. B **563**, 35 (2003).
[5] W. Grimus, M. Maltoni, T. Schwetz, M. A. Tórtola, and J. W. F. Valle, Nucl. Phys. **648**, 376 (2003).
[6] C. Giunti and A. Studenikin, Rev. Mod. Phys. **87**, 531 (2015).
[7] K. Fujikawa and R. E. Shrock, Phys. Rev. Lett. **45**, 963 (1980).
[8] J. Schechter and J. W. F. Valle, Phys. Rev. D **24**, 1883 (1981).
[9] B. Kayser, Phys. Rev. D **26**, 1662 (1982).
[10] J. F. Nieves, Phys. Rev. D **26**, 3152 (1982).
[11] P. B. Pal and L. Wolfenstein, Phys. Rev. D **25**, 766 (1982).
[12] R. E. Shrock, Nucl. Phys. **B206**, 359 (1982).
[13] D. W. Liu *et al.* (Super-KamiokaNDE Collaboration), Phys. Rev. Lett. **93**, 021802 (2004).
[14] C. Arpesella *et al.* (Borexino Collaboration), Phys. Rev. Lett. **101**, 091302 (2008).
[15] A. G. Beda, V. B. Brudanin, V. G. Egorov, D. V. Medvedev, V. S. Pogosov, E. A. Shevchik, M. V. Shirchenko, A. S. Starostin, and I. V. Zhitnikov (GEMMA Collaboration), Phys. Part. Nucl. Lett. **10**, 139 (2013).
[16] G. G. Raffelt, Astrophys. J. **365**, 559 (1990).
[17] S. Arceo-Díaz, K.-P. Schröder, K. Zuber, and D. Jack, Astropart. Phys. **70**, 1 (2015).
[18] C. Patrignani *et al.* (Particle Data Group), Chin. Phys. C **40**, 100001 (2016) and 2017 update.
[19] G. Alimonti *et al.* (Borexino Collaboration), Nucl. Instrum. Methods Phys. Res., Sect. A **600**, 568 (2009).
[20] G. Alimonti *et al.* (Borexino Collaboration), Astropart. Phys. **16**, 205 (2002).
[21] M. Agostini *et al.* (Borexino Collaboration), arXiv: 1707.09279.
[22] G. Belini *et al.* (Borexino Collaboration), Phys. Lett. B **658**, 101 (2008).
[23] G. Bellini *et al.* (Borexino Collaboration), Phys. Rev. Lett. **107**, 141302 (2011).
[24] G. Bellini *et al.* (Borexino Collaboration), Phys. Rev. D **89**, 112007 (2014).
[25] G. Bellini *et al.* (Borexino Collaboration), Nature (London) **512**, 383 (2014).
[26] (Borexino Collaboration) (to be published).
[27] M. Agostini *et al.* (Borexino Collaboration), arXiv: 1704.02291 [Astrophys. (to be published)].
[28] J. N. Abdurashitov *et al.* (SAGE Collaboration), Phys. Rev. C **80**, 015807 (2009).
[29] M. Agostini *et al.* (Borexino Collaboration), Phys. Rev. Lett. **115**, 231802 (2015).
[30] J. F. Beacom and P. Vogel, Phys. Rev. Lett. **83**, 5222 (1999).
[31] A. Joshipura and S. Mohanty, Phys. Rev. D **66**, 012003 (2002).
[32] B. C. Cañnas, O. G. Miranda, A. Parada, M. Tòrtola, and J. W. F. Valle, Phys. Lett. B **753**, 191 (2016); **757**, 568 (2016).
[33] A. S. Dighe, Q. Y. Liu, and A. Yu. Smirnov, arXiv:9903329.